DOI: 10.1002/((please add manuscript number))

Article type: Communication

Cell Behavior within Nanogrooved Sandwich Culture Systems

Isabel M. Bjørge, Manuel Salmeron-Sanchez, Clara R. Correia, João F. Mano**

I. M. Bjørge, Dr. C. R. Correia, Prof. J. F. Mano

CICECO-Aveiro Institute of Materials, Department of Chemistry, University of Aveiro, Campus Universitário de Santiago, 3810-193 Aveiro, Portugal

*E-mails: claracorreia@ua.pt, jmano@ua.pt

Prof. M. Salmeron-Sanchez

Centre for the Cellular Microenvironment, University of Glasgow, Glasgow G12 8LT, UK

Keywords: engineered surface topographies, nanogrooves, sandwich-culture systems, cell orientation, tissue engineering

Grooved topography and inherent cell contact guidance has shown promising results regarding cell proliferation, morphology, and lineage-specific differentiation. Yet these approaches are limited to two-dimensional applications. Sandwich-culture conditions were developed to bridge the gap between two-dimensional and three-dimensional culture, enabling both ventral and dorsal cell surface stimulation. We assess the effect of grooved surface topography on cell orientation and elongation in a highly controlled manner, with simultaneous and independent stimuli on two cell sides. Nanogrooved and non-nanogrooved substrates are assembled into quasi-three-dimensional systems with variable relative

orientations. A plethora of sandwich-culture conditions are created by seeding cells on lower, upper, or both substrates. Software image analysis demonstrates that F-actin of cells acquires the orientation of the substrate on which cells are initially seeded, independently from the orientation of the second top substrate. Contrasting cell morphologies are observed, with a higher elongation for nanogrooved two-dimensional substrates than nanogrooved sandwich-culture conditions. Correlated with an increased pFAK activity and vinculin staining for sandwich-culture conditions, these results point to an enhanced cell surface stimulation versus control conditions. The pivotal role of initial cell-biomaterial contact on cellular alignment is highlighted, providing important insights for tissue engineering strategies aiming to guide cellular response through mechanotransduction approaches.

Cell adhesion is mediated through integrins that tether to extracellular matrix (ECM) proteins, generally associated with an increased actin-myosin contractility to stabilize focal adhesions.[1,2] Integrin-mediated adhesions can be formed on only one cell face or on the entire cell surface in response to a two-dimensional (2D) or three-dimensional (3D) environment, respectively.[3] Therefore, cell morphology, cytoskeletal structure, and signaling are altered for cells cultured on 2D versus 3D environments, as well reported in the literature. For example, in a 2D versus 3D context, cells seeded atop of stiffer hydrogels tend to acquire a spread morphology, whereas cells encapsulated within the same stiff hydrogel are confined and adopt a rounded morphology.[4] As part of the focal adhesion complex, integrins are responsible for mechanotransduction, altering chemical signaling in response to the environment and physical cues to which cells are subjected.[5,6] Downstream signaling initiated by adhesion formation activates distinct pathways, including nuclear or cytoplasmic shuttling of Yorkie-homologues Yes-associated protein (YAP) and transcriptional coactivator with PDZ-binding motif (TAZ). YAP/TAZ have been indicated as sensors and mediators of

mechanical cues, specifically adhesive areas and substrate stiffness, and have thus been linked to geometric control and stiffness-triggered cell differentiation.[7]

By means of contact guidance, topographical features may govern cell orientation, migration, and production of organized cytoskeletal arrangements.[8] There is also evidence that a greater cell deformation by topographical guidance can be correlated with a larger genome response regarding cell cytoskeleton, proliferation, transcription, translation, production of extracellular matrix, as well as inter- and intracellular signaling.[6] For example, larger focal adhesions (>5 mm) and greater actin-myosin contractility with consequent increased intracellular tension have been associated with cell differentiation towards the osteogenic lineage. This is likely due to the transfer of tensile forces to the nucleus, which impacts chromosomal arrangement. Conversely, mesenchymal stromal cells (MSCs) seeded on substrates that restrict spreading and lead to a rounded cell morphology impede the formation of mature adhesions, consequently directing adipogenic differentiation.[2] Other types of cells are also affected by contact guidance, such as pre-osteoblasts,[9] fibroblasts,[10] and myoblasts.[10] Moreover, the use of aligned substrates with different submicron groove and ridge widths has shown promising results in directing the differentiation of MSCs towards osteogenic,[11] adipogenic,[11] myogenic,[12] and chondrogenic [13] lineages. We have recently proposed nanogrooved microdiscs, “topodiscs”, as substrates for cell-mediated assembly structures,[14] which could be used in bottom-up tissue engineering strategies.[15] The osteogenic differentiation of adipose-derived stromal cells (ASCs) even in the absence of osteoinductive factors ascertains the effect of grooved topography in a 3D environment and warrants a more in-depth study of grooved topography.[14]

Sandwich-culture (SW) methods have been applied to bridge the gap between 2D and 3D cultures, allowing for both ventral and dorsal cell surface stimulation.[16–18] When placed in a 3D matrix, dorsal receptor integrins of fibroblasts undergo activation and conformational changes, leading to an altered cell morphology from well-spread to bipolar or stellate.[5] When

placed in a SW, fibroblasts also acquire a stellate morphology, with the formation of smaller and fewer focal adhesions.[18] SW methods have been mainly applied to study the effect of dorsal and ventral protein-loading on cell proliferation, migration, and ECM reorganization.[16,18–20]

With ever-growing evidence that the 2-dimensional approach is not the most appropriate to assess cellular behaviors, we herein propose the production of nanogrooved substrates to be implemented in SW systems, aiming to transpose grooved topography from a 2D to a quasi-3D approach by interacting with both ventral and dorsal cell receptors. Nanogrooved or non-nanogrooved substrates were assembled with different combinations and relative orientations, namely 0º and 90º. MC3T3-E1 pre-osteoblastic cells were seeded on bottom (**Scheme S1**-box 2) or top (Scheme S1-box 3) substrates prior to contact with the second substrate (single-seeded SW) to study the effect of substrate nanogrooves and relative orientation on cell morphology and alignment. Cell seeding on upper substrates was performed to rule out the effect of gravity as cells were allowed to adhere to the upper substrate prior to flipping upside-down onto the lower substrate. It is important to note that regardless the substrate on which cells are seeded (upper or lower), upon closing of the sandwich via placement of the second substrate, the ventral or dorsal substrate will always correspond to the lower or upper substrate, respectively. Additionally, cells were seeded on both substrates (double-seeded SW, Scheme S1-box 4) to evaluate if cell alignment would be affected by the presence of pre-existing cells. We hypothesized that these varying SW conditions would impact cell morphology and alignment due to direct contact with nanogrooved substrates (single-seeded SW) and via promotion of cell-cell contact (double-seeded SW).

To evaluate the effects of the different conditions on cell stimulation and behavior, results were analyzed using both qualitative (**Figure 1**) and quantitative (**Figure 2**) methods. Qualitatively it was observed that for cultures on single substrates, cells either spread randomly on the non-nanogrooved substrate (A) or aligned along the nanogrooves (B), thus

evidencing the influence of substrate topography on cell orientation (Figure 1). Regarding SW conditions (C)-(K) cells generally acquired the morphology of substrates on which they were seeded, independently of the substrate later assembled to produce the SW conditions. Thus, SW conditions with cells seeded on non-grooved substrates (Figure 1 (E), (F), and (K)) tended to acquire a seemingly random orientation, whereas SW conditions with cells seeded on grooved substrates (Figure 1 (C), (D), (G), (H), (I) and (J)) tended to align along a specific direction. This specific orientation was established preferentially according to the initial substrate where cells were seeded, while the opposing substrate seemed to have no effect on cell orientation.

For a quantitative analysis, OrientationJ plug-in for ImageJ was used to create color-coded images of F-actin filament local orientations and translate this data into polar graphs (Figure 2I.). In accordance with the tendency qualitatively observed in Figure 1, in the absence of grooves (condition (A)) cells acquired a random disposition, which was translated into the absence of a peak in the corresponding orientation plot and no dominant color in the image. Conversely, cells cultured on grooved substrates (condition (B)) aligned in a singular direction, which could be observed as a narrow peak and presence of a dominant color in Figure 2I. This cell behavior is also in accordance with previous studies using grooved substrates.[9,10] Regarding SW conditions, the software analysis also corroborated the findings from qualitative data of the disposition of F-actin cytoskeleton (Figure 1), *i.e.* cells aligned according to the groove direction of the substrate on which they were seeded. Cells on grooved substrates (Figure 2I (C), (D), (G), (H), (I) and (J)) tended to align along a dominant direction, whereas cells on non-grooved substrates (Figure 2I (E), (F), and (K)) presented a random distribution. Condition (E) was used as a control SW condition and, as expected, cells presented a random distribution in the absence of nanogrooves. Conditions (C) and (H) with substrates angled at 0º presented a narrow distribution of orientations. Analogously to what Ballester-Beltrán *et al.* [21] observed with cells seeded on aligned fibers with an upper flat

substrate, condition (G) and (J) also presented a narrow distribution of orientations. Curiously, condition (D), and to some extent (I), with substrates angled 90º, presented a narrow distribution of orientations. This occurrence comes to reinforce the importance of initial contact and the finding that cells tend to align according to the substrate on which they were seeded, somewhat independently of further stimuli and also independent of gravity since it was also verified on upper cell-seeded substrates ((H)-(K)). In conditions (F) and (K), cells seeded on non-grooved substrates, placed in contact with opposing grooved substrates, acquired a random orientation. Previous studies did not describe such findings. This might be explained by the fact that MC3T3-E1 cells do not present a radial branching morphology[21] , contrarily to other cell types used in such studies, such as C2C12 and fibroblasts. Additionally, we have mapped cellular orientation based on the alignment of actin filaments, and not the orientation of the cell body by cytoplasmic staining, as has been described in previous works.[10,21] Therefore, our study highlights relevant findings that should be considered when designing surface engineering strategies aiming to control cell behavior.

Even though the formation of focal adhesions is a dynamic process, the initial three-hour adhesion time prior to closing the SW proves to be crucial on regulating cell morphology. It has been previously shown that if this initial step is bypassed, the elongation of cells is jeopardized, and consequently a rounded morphology is acquired. This is in fact a limitation of the system, indicating that cell spreading is affected within SWs and that opposing substrate stimulation can only partially affect cell morphology.[22] In the assessed SW condition, a higher density in the activation of vinculin sites could be observed when compared to control single substrate condition, as shown in Figure 2II. The increased vinculin staining for SW condition (C) comparatively with control 2D-condition (B) may in fact be attributed to an enhanced engagement of the cell surface. Taking into consideration a previous SW culture study where upper substrate weight was deemed as not responsible for cell morphological changes,[18] this augmented engagement expectedly results from the effective

contact of the cells to both substrates. However, since we did not directly assess the effects of varying substrate weight, we should consider that it may be driven by a greater ventral stimulation. Either way, these results confirm the greater stimulation within SW and corroborate our hypothesis. This is an important outcome for SW systems, since vinculin has recently emerged as a major player in focal adhesions-mediated mechanotransduction, facilitating 3D cell migration.[23] Even though focal adhesions have been extensively studied in 2D, studies in 3D such as cell encapsulation within hydrogels have yielded contradictory findings [24,25]. It has been previously proposed that focal and fibrillar adhesions observed in 2D studies are an amplification of *in vivo* 3D matrix adhesions.[26] Whereas the present study is not performed using a 3D model, it is a step further concerning 2D studies. When comparing the expression of focal adhesion kinase and its phosphorylation at Tyr-397 for control grooved condition (B) and SW condition (C), results showed a comparable FAK expression for both samples yet a significantly enhanced pFAK expression was observed for the SW condition (Figure 2III). Phosphorylation of FAK at Tyr-397 occurs upon integrin binding, denoting downstream signaling followed by integrin-mediated adhesion for the SW condition. Disassembly of integrin-based adhesion sites has in turn been linked to FAK signaling, indicating an equal degree of focal adhesion turnover, which has been linked to cell migration.[27,28] In accordance with a previous work that compared FAK and pFAK expression on fibroblasts cultured in regular 2D conditions and SW conditions, it was observed that the pFAK/FAK ratio was enhanced in SW culture conditions where cells were allowed to adhere for 3h prior to SW closing, as was performed in this study.[19] Taking together both the increased vinculin site activation and pFAK expression for SW condition (C) comparatively to nanogrooved control-2D condition (B), the enhanced interaction provided by simultaneous dorsal and ventral stimulation of the cell surface is here demonstrated.

Cell elongation was another studied morphological aspect, corresponding to the ratio between the longest cell axis measured and the maximal perpendicular length. Grooved control

condition (B) presented the highest elongation factor, followed by SW condition (C) with a 0º orientation angle between lower and upper substrates (Figure 2III). As expected, conditions (E), (F), and (K), where cells were seeded on non-patterned substrates, elongated the least. For these cases, cells were not subject to contact guidance and thus spread randomly on the substrate. Interestingly, grooved sandwich conditions (C), (D), (H), (I), and (J) presented a lower elongation factor than patterned control (B), even if not statistically significant for every condition. This may be due to the conjoint effect of ventral and dorsal stimuli, where cell spreading also occurs vertically, bridging both upper and lower substrates and acquiring an hourglass-like shape.[29] Comparatively to previously performed studies, Ballester-Beltrán *et al.* also observed alterations in morphology for fibroblasts seeded within sandwich conditions, comparatively to regular 2D conditions.[22] Therefore, although little or no effect was qualitatively found for cell orientation, cell elongation was actively affected.

Subsequently and in order to determine whether the presence of cells on both upper and lower substrates could be another influencing factor on cell behavior, double-seeded SW conditions were also studied. Cells stained with either DiO (green) or DiD (red) were seeded on independent substrates and closed onto each other for cells on both substrates to come in contact. Upon the disassembling of SW conditions, it was observed that few cells migrated from the upper substrate to the lower substrate but none in the opposite direction; moreover, migrated cells (green) acquired a similar orientation to pre-seeded cells (red) (**Figure S1**). By confocal microscopy of closed double-seeded SW conditions, the relative orientation of substrates could be observed, as well as the integration of cells from both substrates on one plane, further confirming contact between upper and lower substrates (**Figure 3**I; **Figure S2** illustrates the scenario when contact between substrates was not obtained). Cytoplasmic staining proved not to be sufficiently detailed for the development of rigorous orientation maps; thus, F-actin staining of conditions (L)-(N) was performed to obtain a precise cell mapping (Figure 3II). Similarly to single-seeded conditions, cells acquired the orientation of

the substrate on which they were seeded. A narrow distribution of orientation could be observed for both lower and upper substrates of condition (M), which were angled at 0º. For condition (L), with a lower substrate presenting no grooves, or condition (N) with substrates angled at 90º, no significant differences were observed in cell orientation. For both conditions, cells initially seeded on grooved substrates aligned accordingly or spread randomly on non-grooved substrates.

When comparing single versus double-seeding, single-seeded conditions (G) and (J) and double-seeded condition (L) have grooved substrates versus non-grooved substrates, yet a greater alignment was found for condition (J) than for (G), which was similar to (L). With the same groove orientation, double-seeded condition (M) presented a narrow distribution of orientation, as was verified for conditions (C) and (H). When considering a 90º angle orientation between substrates, condition (N) also presented a narrow distribution, similarly to single-seeded conditions (D) and (I). In condition (L), cells on the lower non-grooved substrate presented a random distribution, whereas cells on the upper grooved substrate presented a definite trend towards a certain orientation, similarly to condition (G), even if not as narrow as condition (J).

In conclusion, we proposed a sandwich culture model featuring varying combinations of nanogrooved topography on lower and upper substrates, with varying angles of nanogroove orientation between substrates, featuring single or double-seeding. For both single and double-seeded conditions, cells tended to acquire the orientation of the substrate on which they were seeded, evidencing the influence of initial contact over further stimuli from opposing substrates. Furthermore, cell elongation was effectively altered within SW conditions versus control 2D substrates, even if substrate orientation was not an impacting factor. This study explores for the first time the effect of nanogrooves on dorsal and ventral cell receptors under highly controlled orientation conditions, highlighting the significant impact of initial contact on cell morphology and orientation. Moreover, this is noteworthy for

tissue engineering strategies focusing on surface engineering, in particular on surface topography, as it brings new light into the role of the initial contact on cell behavior. Hence, even upon degradation or replacement of the biomaterial, the initial response of cells to the material may have an important influence on its bioperformance. We envision that a widespread application of SW cultures to distinct substrate materials, including soft materials (e.g. hydrogels), may deliver valuable information regarding the effects of mechanical cues on cells by combining stiffness and topography cues in an engineered quasi-3D environment more realistic compared to the conventional 2D platforms, and emphasize the contribution in the field of regenerative medicine through the development of mechanobiology platforms.

Experimental Section

Sandwich cell culture: MC3T3-E1 cells (American Type Culture Collection) were cultured with α-MEM supplemented with 10% fetal bovine serum (ThermoFisher Scientific) and 1% antibiotic-antimycotic (100x, ThermoFisher Scientific) in tissue culture flasks, incubated at 37ºC in a humidified air atmosphere of 5% CO_2. At 90% confluence, cells were detached by 0.05 % w/v trypsin-EDTA (from porcine pancreas 1:250, Sigma-Aldrich) treatment for 5 min at 37ºC. Cells were carefully seeded to avoid bubble formation at a density of $1.5x10^4$ cells/cm^2 and allowed to adhere for 3 h at 37ºC. SW conditions are produced by assembling nanogrooved or non- nanogrooved substrates with or without cells, and with variable relative orientations (0º or 90º) between nanogrooves of upper and lower substrates. Additionally, SW conditions with cells seeded on both lower and upper substrates were tested where MC3T3-E1 cells were incubated with DiO (Vybrant® DiO Cell-Labelling Solution, ThermoFisher Scientific) or DiD (Vybrant® DiD Cell-Labelling Solution, ThermoFisher Scientific) for 30 minutes at 37ºC (5 μL of dye per mL of cell suspension containing $1x10^6$ cells). Stained cells were seeded on respective substrates ($1x10^4$ cells/cm^2) and left to adhere for 3 hours at 37ºC. SW conditions were produced by assembling DiO-stained cell-seeded upper substrates with

DiD-stained cell-seeded lower substrates. Contact between upper and lower substrates was ensured by placing a glass substrate (10x5x1 mm; 150 mg) over assembled SWs. For all assessed conditions, upon the initial 3h adhesion period, cells were cultured for 21h on single substrates or within the SW, totaling 24h of culture. **Scheme S1** available as supplementary information shows the different assembly conditions tested.

Supporting Information
Supporting Information is available from the Wiley Online Library or from the author.

Acknowledgements
I. M. Bjørge acknowledges financial support by the Portuguese Foundation for Science and Technology (FCT) with doctoral grant SFRH/BD/129224/2017. This work was supported by the European Research Council grant agreement for the project "ATLAS" (ERC-2014-ADG-669858) and the FCT project "CIRCUS" (PTDC/BTM-MAT/31064/2017). This work was developed within the scope of the project CICECO-Aveiro Institute of Materials, UIDB/50011/2020 & UIDP/50011/2020, financed by national funds through the FCT/MEC and when appropriate co-financed by FEDER under the PT2020 Partnership Agreement. Image acquisition was performed in the LiM facility of iBiMED, a node of PPBI (Portuguese Platform of BioImaging): POCI-01-0145-FEDER-022122. This work was supported by an EPSRC Programme Grant (EP/P001114/1, Engineering growth factor microenvironments - a new paradigm for regenerative medicine)"

Received: ((will be filled in by the editorial staff))
Revised: ((will be filled in by the editorial staff))
Published online: ((will be filled in by the editorial staff))

References

[1] A. I. Alford, K. M. Kozloff, K. D. Hankenson, *Int. J. Biochem. Cell Biol.* **2015**, *65*, 20.

[2] H. Donnelly, M. Salmeron-Sanchez, M. J. Dalby, *J. R. Soc. Interface* **2018**, *15*, 20180388.

[3] B. M. Baker, C. S. Chen, *J. Cell Sci.* **2012**, *125*, 3015.

[4] S. R. Caliari, S. L. Vega, M. Kwon, E. M. Soulas, J. A. Burdick, *Biomaterials* **2016**, *103*, 314.

[5] M. Larsen, V. V Artym, J. A. Green, K. M. Yamada, *Curr. Opin. Cell Biol.* **2006**, *18*, 463.

[6] M. J. Dalby, *Med. Eng. Phys.* **2005**, *27*, 730.

[7] S. Dupont, L. Morsut, M. Aragona, E. Enzo, S. Giulitti, M. Cordenonsi, F. Zanconato, J. Le Digabel, M. Forcato, S. Bicciato, N. Elvassore, S. Piccolo, *Nature* **2011**, *474*, 179.

[8] R. G. Flemming, C. J. Murphy, G. A. Abrams, S. L. Goodman, P. F. Nealey, *Biomaterials* **1999**, *20*, 573.

[9] K. Wang, L. Cai, L. Zhang, J. Dong, S. Wang, *Adv. Healthc. Mater.* **2012**, *1*, 292.

[10] M. P. Sousa, S. G. Caridade, J. F. Mano, *Adv. Healthc. Mater.* **2017**, *6*, 1601462.

[11] G. Abagnale, M. Steger, V. H. Nguyen, N. Hersch, A. Sechi, S. Joussen, B. Denecke, R. Merkel, B. Hoffmann, A. Dreser, U. Schnakenberg, A. Gillner, W. Wagner, *Biomaterials* **2015**, *61*, 316.

[12] P.-Y. Wang, W.-T. Li, J. Yu, W.-B. Tsai, *J. Mater. Sci. Mater. Med.* **2012**, *23*, 3015.

[13] Y.-N. Wu, J. B. K. Law, A. Y. He, H. Y. Low, J. H. P. Hui, C. T. Lim, Z. Yang, E. H. Lee, *Nanomedicine Nanotechnology, Biol. Med.* **2014**, *10*, 1507.

[14] I. M. Bjørge, I. S. Choi, C. R. Correia, J. F. Mano, *Nanoscale* **2019**, 16214.

[15] V. M. Gaspar, P. Lavrador, J. Borges, M. B. Oliveira, J. F. Mano, *Adv. Mater.* **2020**, *32*, 1903975.

[16] J. C. Dunn, M. L. Yarmush, H. G. Koebe, R. G. Tompkins, *FASEB J.* **1989**, *3*, 174.

[17] Y. Y. Gong, J. X. Xue, W. J. Zhang, G. D. Zhou, W. Liu, Y. Cao, *Biomaterials* **2011**, *32*, 2265.

[18] K. A. Beningo, M. Dembo, Y. Wang, *Proc. Natl. Acad. Sci. U. S. A.* **2004**, *101*, 18024.

[19] J. Ballester-Beltrán, D. Moratal, M. Lebourg, M. Salmerón-Sánchez, *Biomater. Sci.* **2014**, *2*, 381.

[20] J. Ballester-Beltrán, M. Lebourg, P. Rico, M. Salmerón-Sánchez, *Nanomedicine* **2015**, *10*, 815.

[21] J. Ballester-Beltrán, M. Lebourg, M. Salmerón-Sánchez, *Biotechnol. Bioeng.* **2013**, *110*, 3048.

[22] J. Ballester-Beltrán, M. Lebourg, P. Rico, M. Salmerón-Sánchez, *Biointerphases* **2012**, *7*, 1.

[23] T. Omachi, T. Ichikawa, Y. Kimura, K. Ueda, N. Kioka, *PLoS One* **2017**, *12*, e0175324.

[24] K. E. Kubow, A. R. Horwitz, *Nat. Cell Biol.* **2011**, *13*, 3.

[25] S. I. Fraley, Y. Feng, R. Krishnamurthy, D.-H. Kim, A. Celedon, G. D. Longmore, D. Wirtz, *Nat. Cell Biol.* **2010**, *12*, 598.

[26] E. Cukierman, R. Pankov, D. R. Stevens, K. M. Yamada, *Science.* **2001**, *294*, 1708.

[27] A. Hamadi, M. Bouali, M. Dontenwill, H. Stoeckel, K. Takeda, P. Rondé, *J. Cell Sci.* **2005**, *118*, 4415.

[28] S. K. Mitra, D. A. Hanson, D. D. Schlaepfer, *Nat. Rev. Mol. Cell Biol.* **2005**, *6*, 56.

[29] O. Chaudhuri, S. H. Parekh, W. A. Lam, D. A. Fletcher, *Nat. Methods* **2009**, *6*, 383.

[30] R. Rezakhaniha, A. Agianniotis, J. T. C. Schrauwen, A. Griffa, D. Sage, C. V. C. Bouten, F. N. van de Vosse, M. Unser, N. Stergiopulos, *Biomech. Model. Mechanobiol.* **2012**, *11*, 461.

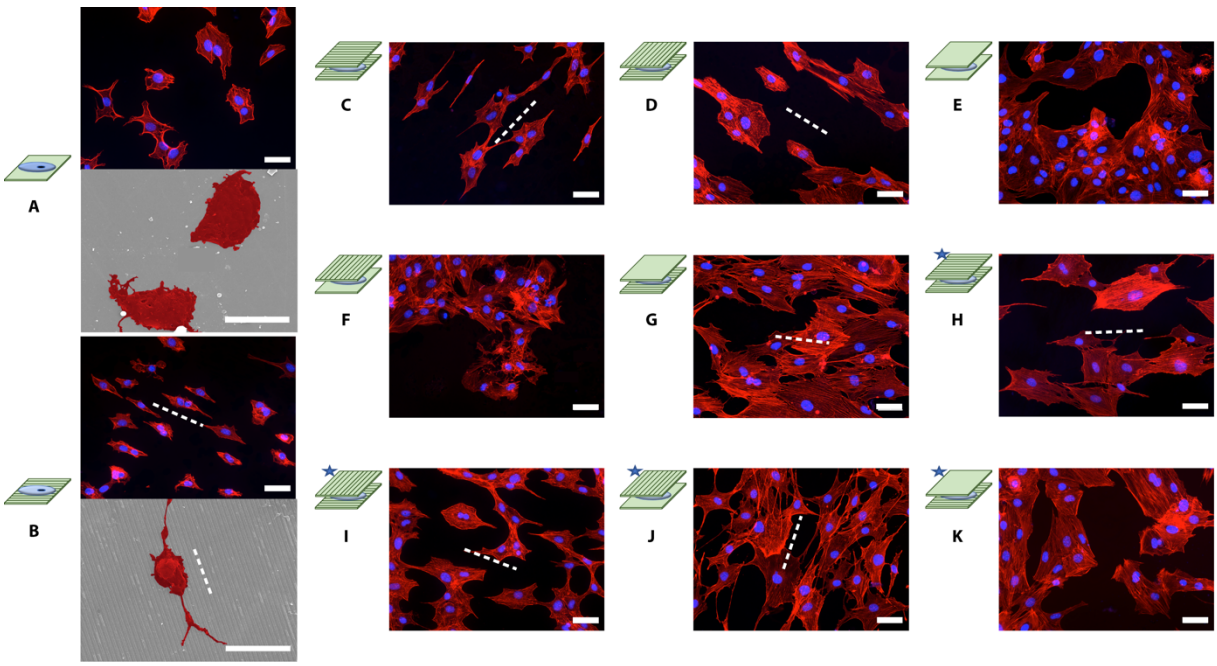

Figure 1. MC3T3-E1 cells seeded on 2D substrates or in SW conditions. F-actin stained in red and cell nuclei in blue. Cells seeded on lower substrates unless marked with a star. Images correspond to the substrate where cells were seeded (50 µm scale bars). Cells painted in red in SEM images for conditions (A) and (B) (20 µm scale bars). White dotted lines indicate nanogroove orientation of cell seeded substrates.

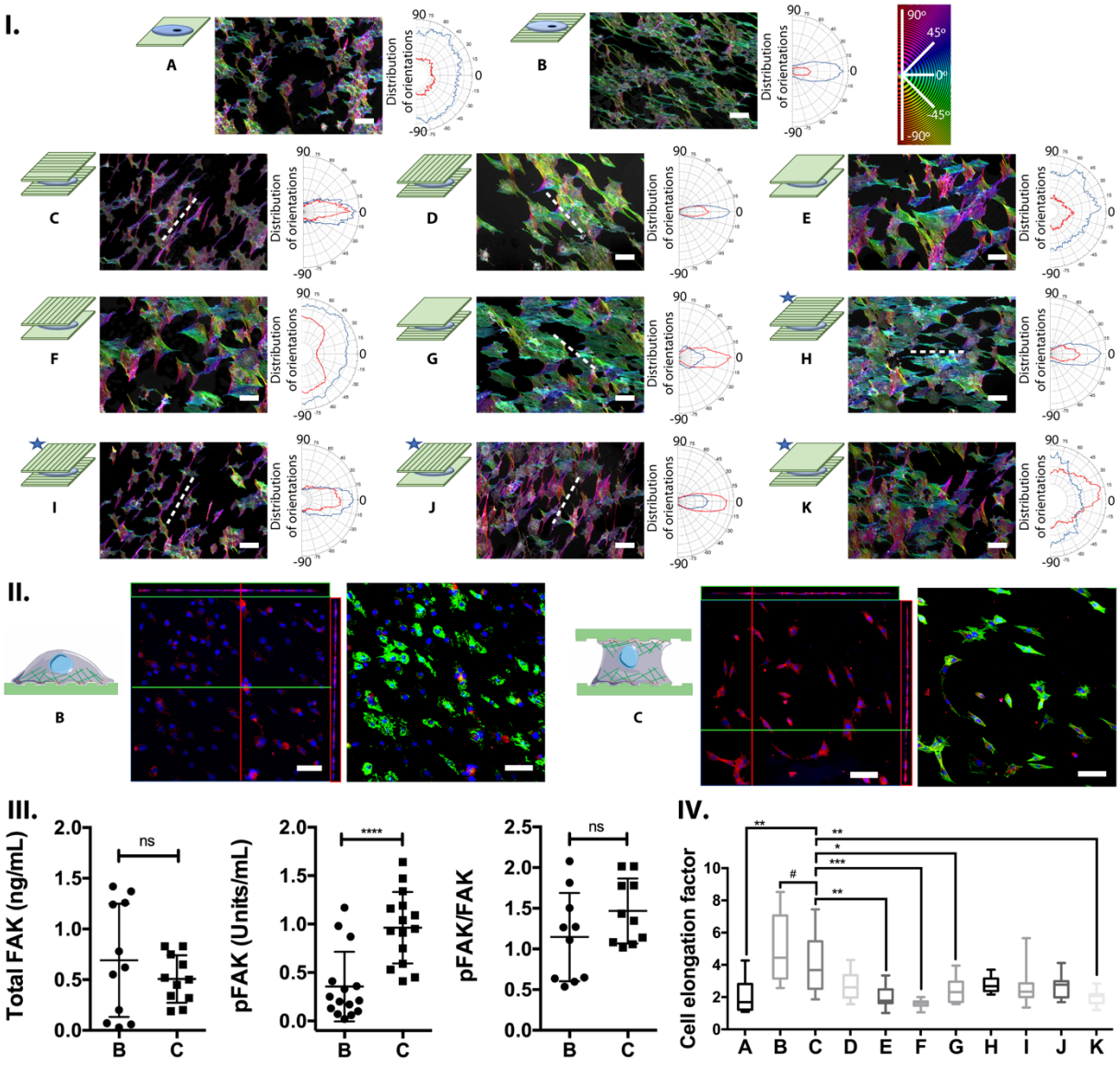

Figure 2. Analysis of 2D substrates ((A) and (B)) and single-seeded SW conditions ((C)-(K)). I. Orientation color-coded F-actin and corresponding orientation plots (n=2), ranging from -90 to 90º (circular color-coding map inset) (100 µm scale bars). Cells seeded on lower substrates unless marked with a star. White dotted lines indicate nanogroove orientation of cell seeded

substrates. II. Cells for conditions (B) and (C) stained with vinculin (red) and nuclei (blue), with corresponding orthogonal views (left) and counterstaining of F-actin in green (right). III. Quantification via ELISA of total FAK (ng/mL) and phosphorylation of FAK at Tyr-397 (units/mL) for conditions (B) and (C) (n≥11) with corresponding pFAK/FAK ratio. Statistical significance of p≤0.0001 (****). IV. Cell elongation factor (n≥8). Statistical significance of p≤0.05 (*), p≤0.01 (**) and p≤0.001 (***) are represented when applicable. Statistical significance was observed between condition (B) and every other condition except (C), represented with # to facilitate reading.

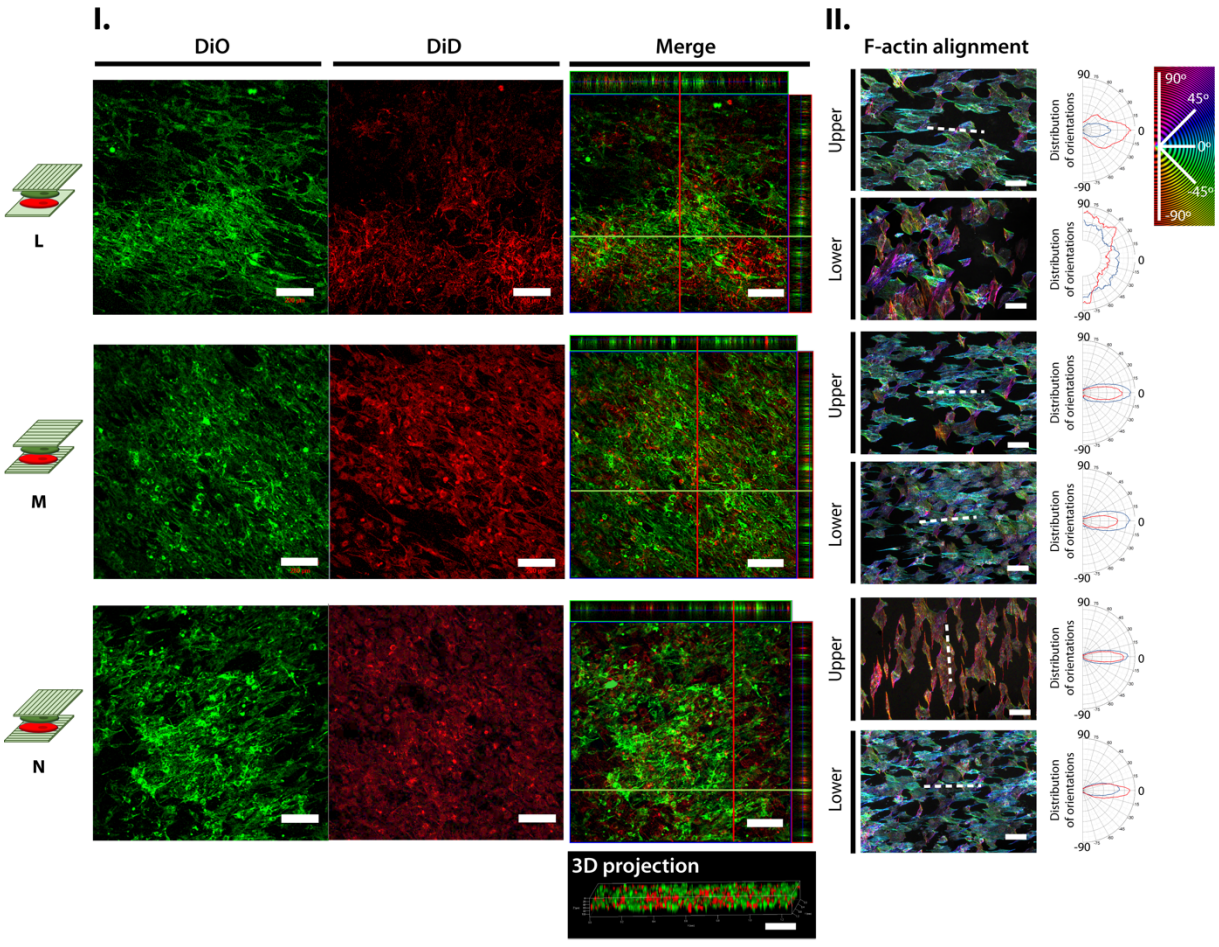

Figure 3. Double-seeded SW conditions (L)-(N) (100 µm scale bars). I. Confocal images of closed sandwich conditions: DiO (green) and DiD (red) stained cells, previously seeded on upper and lower substrates, respectively, with corresponding channel merging and orthogonal

views. 3D projection of condition (L). II. Open SW orientation color-coded F-actin and corresponding orientation plots (n=2), ranging from -90 to 90º (circular color-coding map inset). White dotted lines indicate nanogroove orientation.

Nanogrooved sandwich-culture systems with relative orientation to assess cell response while stimulating cell dorsal and ventral receptors, featuring single and double-seeded substrates. Cells acquire the orientation of the substrate on which they are initially seeded, independently of the orientation or existence of pre-seeded cells on opposing substrates, whereas cell elongation is effectively conditioned within SW.

Sandwich-culture systems

I. M. Bjørge, M. Salmeron-Sanchez, C. R. Correia,* J. F. Mano*

Cell Behavior within Nanogrooved Sandwich Culture Systems

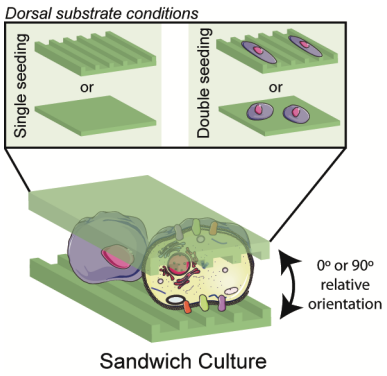

Supporting Information

Cell Behavior within Nanogrooved Sandwich Culture Systems

Isabel M. Bjørge, Manuel Salmeron-Sanchez, Clara R. Correia, João F. Mano**

Experimental section

Micromolding of polystyrene substrates: Polystyrene adherent petri dishes (Plate Cell + 150, Sarstedt) were cut into 8 x 8 mm^2 substrates using a laser-cutting machine (Ignis, BCN3D). Optical media substrates (CDs; ridge width 1185±16 nm, groove width 412±12 nm, and ridge height 197±14 nm) were used as nanogrooved templates to mold polystyrene substrates. Molding was performed in an oven (Ecocell 55, MMM Medcenter Einrichtungen GmbH) at 120ºC for 50 minutes with an applied pressure of approximately 130 mPa. Polystyrene substrates were plasma treated (Plasma System ATTO, Electronic Diener) at 0.4-0.6 mbar and 30 V for 15 min using atmospheric air, followed by UV sterilization during 30 min.

Scanning electron microscopy: The nanogrooved surface of substrates and cells was imaged by scanning electron microscopy (SEM; S4100, Hitachi). Cell-seeded substrates were prepared as follows: fixation in 4 % v/v formaldehyde solution (Sigma-Aldrich) in phosphate buffered saline (PBS, Corning) for 30 min at RT, followed by dehydration in increasing ethanol series (60, 70, 80, 90, 96, and 100 wt %, Fisher Chemical) for 10 min at RT in each solution. Lastly, samples were sputtered with gold-palladium.

Fluorescence microscopy: DAPI (4',6-diamidino-2-phenylindole, dihydrochloride, 1 mg/mL, ThermoFisher Scientific) and phalloidin (Flash Phalloidin™ Red 594, 300U, BioLegend) were used to stain cell nuclei in blue and F-actin in red, respectively. Samples were fixed in 4% v/v formaldehyde solution (30 min at RT) and permeabilized in 0.1 % v/v triton-X100 (BioXtra, Sigma-Aldrich) (5 minutes at RT). Samples were incubated in phalloidin-red solution diluted in PBS (5:200) for 45 min at RT, protected from light, and counterstained with DAPI solution diluted in PBS (1:1000) for 5 min at RT protected from light. For vinculin immunofluorescence, samples were incubated in 5% v/v FBS in PBS (5% FBS/PBS) for 1h at RT upon fixation and permeabilization. Cells were incubated with primary antibody (Vinculin Antibody 42H89L44, ABfinity™ Rabbit Monoclonal, 0.5 mg/mL, ThermoFisher Scientific) diluted in 5% FBS/PBS (1:50) overnight at 4ºC. Samples were then incubated with secondary antibody (Alexa Fluor® 594 Donkey anti-rabbit IgG Antibody, BioLegend) diluted in 5% FBS/PBS (1:500). Lastly, F-actin and nuclei were stained as mentioned above with phalloidin (Flash Phalloidin™ Green 488, 300U, BioLegend) and DAPI. Samples were analyzed by fluorescence microscopy (Axio Imager 2, Zeiss) and confocal fluorescence microscopy (LSM 880, Zeiss).

Total FAK and FAK Y397 phosphorylation quantification: Conditions (B) and (C) were prepared as described above. Cell pellets were extracted using cell extraction buffer (Pierce RIPA Buffer, Thermo Scientific) and frozen at -80ºC. FAK (Total) Elisa Kit and FAK (Phospho) [pY397] Human ELISA Kit (ThermoFisher Scientific) were used for quantification.

Cell morphology characterization: OrientationJ plug-in for ImageJ was used to study the orientation of F-actin in fluorescence images. OrientationJ Analysis submenu was used to create a color-survey of images according to the local orientation. An orientation histogram

was created using the Distribution submenu, where a minimum energy of 2% was set in order to remove the background signal.[30] Cell dimensions were measured using ImageJ to calculate the average elongation factor for each condition (Equation (1)).

Elongation factor=Longest cell axisMaximal length perpendicular to longest axis

(1)

Statistical analysis: Statistical analysis was performed using one-way analysis of variance (ANOVA) with Tukey's multiple comparisons test, or Mann-Whitney U test (GraphPad Prism 6.0) A p-value < 0.05 was considered statistically significant.

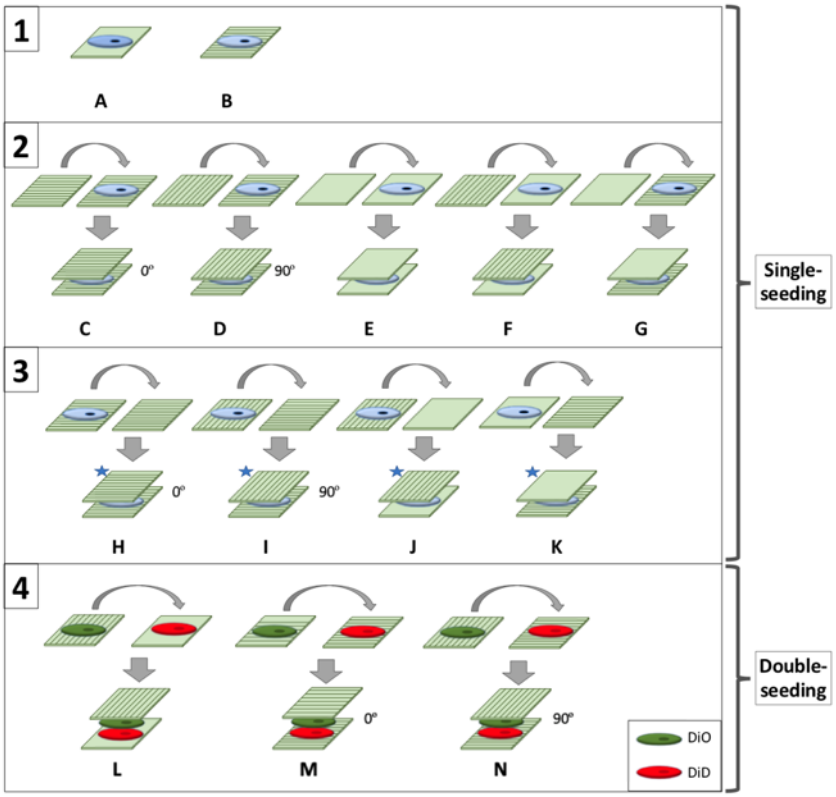

Scheme S1. Schematic representation of the different assembly conditions tested. MC3T3-E1 cells were seeded on polystyrene substrates with or without grooves and placed in sandwich-culture (SW) conditions. Cell seeding was performed on lower substrates unless marked with a star symbol. Relative orientations correspond to the angle between the nanogrooves of the

upper and lower substrates. [Box 1] Control conditions without (A) or with (B) nanogrooves. [Box 2] SW conditions with cell-seeded lower substrates (single-seeding). The orientation of the nanogrooves between the upper and lower substrates is varied between 0º (C) and 90º (D). SW conditions with both substrates without nanogrooves (E) or presenting the nanogrooves on the upper (F) or lower (G) substrate. [Box 3] SW conditions with cell-seeded upper substrates (single-seeding). SW conditions with relative orientation of 0º (H) or 90º (I), and upper (J) or lower (K) grooved substrates. [Box 4] SW conditions with cell-seeded upper and lower substrates (double seeding). Cells adhered to upper or lower substrates are stained with DiO (green) or DiD (red) lipophilic dyes, respectively. SW conditions with the grooves only on the upper substrate (L), or with relative orientations of 0º (M) or 90º (N).

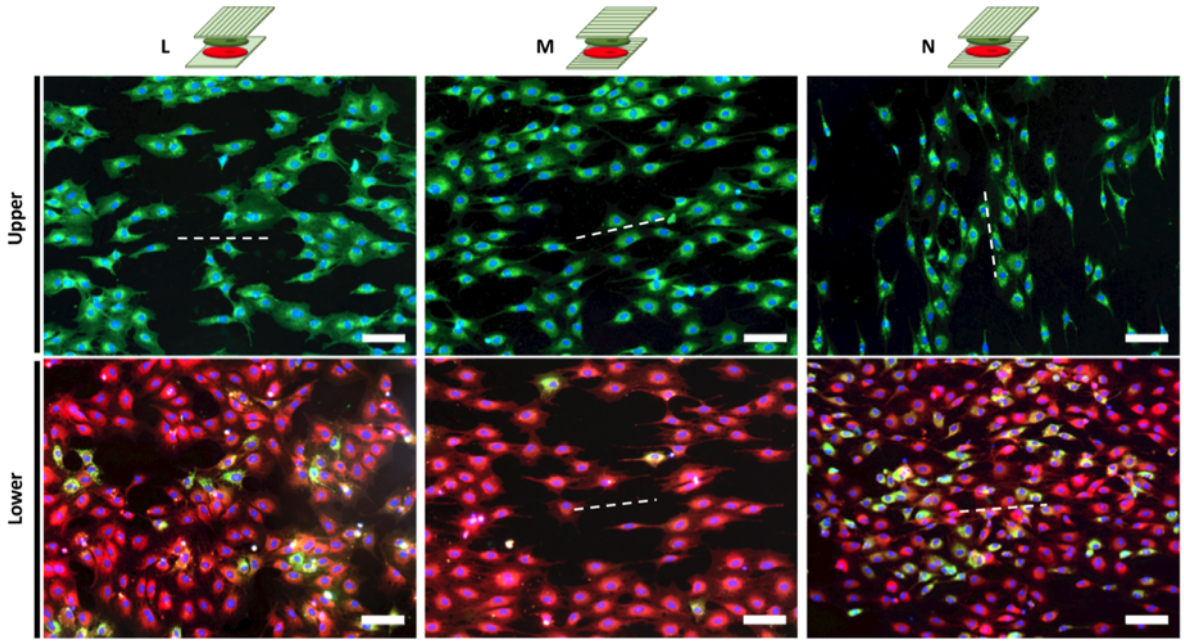

Figure S1. Fluorescence images of SW conditions (L), (M), and (N) demonstrating the relative orientation of cells seeded on upper and lower substrates stained with DiO (green) and DiD (red), respectively. Some cells from the upper substrate tend to migrate and attach more firmly to the lower substrate, yet the opposite does not occur. Scale bars correspond to 200 μm.

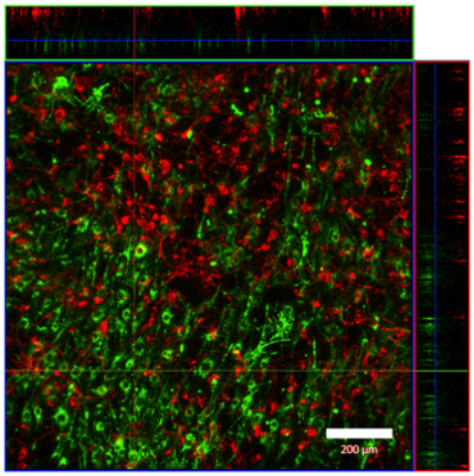

Figure S2. Fluorescence confocal image of cells seeded in a closed SW condition stained with DiO (green) and DiD (red) for upper and lower substrates, respectively. Along the *z* axis it is possible to observe that cells from distinct substrates are in fact not in contact and opposing substrate stimulation will not impact cell behavior. In order to guarantee substrate contact, additional measures were taken to prevent this occurrence. Scale bar corresponds to 200 µm.